Anal Bioanal Chem (2016) 408:1557–1564
DOI 10.1007/s00216-015-9228-7

RESEARCH PAPER

# Identification of a novel mitochondrial interacting protein of C1QBP using subcellular fractionation coupled with CoIP-MS

**Ruibing Chen**[1] · **Mingming Xiao**[1] · **Huajun Gao**[1] · **Yajing Chen**[1] · **Yongmei Li**[1] · **Yunde Liu**[1] · **Ning Zhang**[1]

Received: 24 September 2015 / Revised: 3 November 2015 / Accepted: 27 November 2015 / Published online: 11 January 2016


**Abstract** The study of protein-protein interactions is an essential process to understand the biological functions of proteins and the underlying mechanisms. Co-immunoprecipitation coupled with mass spectrometry (CoIP-MS) is one of the most extensively used high-throughput techniques to discover novel protein-protein interactions. However, the traditional CoIP process uses whole cell lysate, disrupts cellular organization, and leads to potential false positives by inducing artificial protein-protein interactions. Here, we have developed a strategy by combining subcellular fractionation with CoIP-MS to study the interacting proteins of the complement component 1, q subcomponent binding protein (C1QBP) in the mitochondria. Using this method, a novel C1QBP interacting protein, dihydrolipoyllysine-residue acetyltransferase component of pyruvate dehydrogenase complex, mitochondrial (DLAT) was identified and validated. Furthermore, the activity of the pyruvate dehydrogenase (PDH) was found to be affected by the expression level of C1QBP. These results provide novel insights regarding the mitochondrial function of C1QBP in the regulation of cellular energy metabolism. This method could also be used to analyze the subcellular protein-protein interactions for other proteins of interest.

**Keywords** CoIP-MS/MS · C1QBP · LC-MS/MS · Mitochondria · Protein-protein interaction · Subcellular fractionation

## Introduction

The primary DNA sequences from a large variety of species have become available in the last two decades, thanks to high-throughput genome sequencing projects. However, the functions of the majority of the predicted genes remain unclear. Proteins exert their biological activities in a highly coordinated fashion. Hence, the study of protein-protein interactions has become an essential process to understand their functions and the underlying mechanisms. Co-immunoprecipitation coupled with mass spectrometric identification (CoIP-MS) is one of the most widely used techniques to reveal novel protein-protein interactions [1, 2]. To isolate interacting proteins using co-immunoprecipitation, typically an antibody specific for the target protein is incubated with the cell lysate to form immune complexes, which are isolated using immobilized protein A or protein G beads. However, the cellular localizations of proteins are disrupted in this process, which could induce artificial protein-protein interactions. Unlike non-specific binding proteins introduced by the antibody or the affinity solid phase support, this type of false positive cannot be eliminated by quantitative proteomics [3, 4]. Therefore, subcellular fractionation has been suggested to be performed prior to CoIP-MS in order to improve the accuracy of the identification [1]. In addition, fractionating the cellular proteins before CoIP-MS may

Ruibing Chen, Mingming Xiao and Huajun Gao contributed equally to this work.

**Electronic supplementary material** The online version of this article (doi:10.1007/s00216-015-9228-7) contains supplementary material, which is available to authorized users.

✉ Ruibing Chen
chenruibing@tijmu.edu.cn

✉ Ning Zhang
zhangning@tijmu.edu.cn

[1] Tianjin Medical University Cancer Institute and Hospital, National Clinical Research Center for Cancer, Key Laboratory of Cancer Prevention and Therapy; Research Center of Basic Medical Sciences; School of Medical Laboratory, Tianjin Medical University, Tianjin 300070, China

reduce the sample dynamic range and increase the detection sensitivity. However, the potential of such a strategy has yet to be explored.

The complement component 1, q subcomponent binding protein (C1QBP/p32/HABP1) is an acidic protein that can bind with the complement component C1q and is designated the gC1q receptor [5–7]. Its mature form contains 74–282 amino acid residues, which is generated by the removal of the N-terminal mitochondria targeting sequence (1–73 aa residues) during post-translational processing [7]. C1QBP is a multifunctional protein reported to be related with immune response, metabolism, cancer progression, and metastasis, among many others [8–14]. It can be detected in the cytosol, cell surface, and nucleus of different cells, but mostly in the mitochondria [7, 13, 15]. Although C1QBP is normally referred to as a mitochondrial protein, its functions in the mitochondria are still largely unclear. In our previous study, the interactome of C1QBP was established using dimethylation stable isotopic labeling and 2D LC-MS/MS [14]. Although C1QBP is predominantly localized in the mitochondria, the majority of the identified C1QBP interacting proteins are from the cytoplasm [14]. Further in-depth investigation is required to characterize its interacting proteins in the mitochondria, which is crucial to understand why C1QBP is translocalized to the mitochondria and what roles it plays. In this study, mitochondrial C1QBP interacting proteins were investigated combining subcellular fractionation, co-immunoprecipitation, chemical crosslinking, SDS-PAGE, and LC-MS/MS.

## Experimental

### Antibodies and reagents

Dithiothreitol (DTT), iodoacetamide (IAA), and Janus Green B were from Sigma Aldrich (St. Louis, MO). Rabbit anti-C1QBP polyclonal antibody and mouse anti-β-actin monoclonal antibody, and normal rabbit IgG were from Santa Cruz (Santa Cruz, CA); mouse monoclonal antibody against dihydrolipoyllysine-residue acetyltransferase component of pyruvate dehydrogenase complex, mitochondrial (DLAT) was bought from Cell Signaling Technology (Beverly, MA); rabbit polyclonal antibody against cytochrome *c* oxidase polypeptide IV (COX-IV) was from ProteinTech (Chicago, IL). Crosslinking reagent disuccinimidyl suberate (DSS), enhanced chemiluminescence reagents, Lipofectamine 2000, BCA reagents, Protein A agarose beads, and Dynabeads Protein A were purchased from Life Technologies (Carlsbad, CA). Protease Inhibitor Cocktail tablets were purchased from Roche Diagnostics (Indianapolis, IN). Sequencing grade modified trypsin was purchased from Promega (Madison, WI).

### Cell culture, plasmid, shRNA, and transfection

The HEK293T human embryonal kidney cell line, 786-O renal cancer cell line, and ACHN renal cancer cell line used in this study were obtained from American Type Culture Collection. Cells were cultured in DMEM supplemented with 10 % fetal bovine serum and 1 % glutamine Pen-Strep solution at 37 °C and 5 % $CO_2$. For C1QBP knockdown, shRNA sequences targeting C1QBP (5′-GAAGGCCCTTGTGTTGGACTGTCAT-3′; 5′-ACTGGCGAGTCTGAATGGAAGGATA-3′; 5′-GACTGGGCCTTATATGACCACCTAA-3′) were annealed and ligated into the lentivirus vector (pLK0.1-TRC), and retrovirus packaging and infection were carried out. For C1QBP overexpression, lentivirus plasmid vector pCDH-CMV-MCS-EF1-Puro was used for infection. For stable clones, virally infected cells were cultured in medium containing 2.5 μg/mL puromycin for about 10 days, and the drug-resistant clones were collected and expanded. The expression levels of C1QBP in the stable cell lines were evaluated using real-time PCR and Western blotting.

### Mitochondria purification

Mitochondria from HEK293T cells were isolated using the sucrose centrifugation method modified from a protocol described by Dimauro et al. [16]. Briefly, HEK293T cells were washed with chilled PBS, resuspended in 400 μL RSB buffer (10 mM NaCl, 2.5 mM $MgCl_2$, 10 mM Tris-Cl pH=7.4), and kept on ice for 10 min. Three different methods were compared for cell disruption: (1) cells in a 1.5-mL Eppendorf tube were placed in ice and sonicated three times (duration 1 s, pulse 30 s, energy 10 %); (2) cells were transferred to a 2-mL glass tissue homogenizer and ground with the pestle for about ten times; (3) cells were homogenized by passing repeatedly through a needle (0.33×13 mm) attached to a 1-mL syringe. Then 200 μL 3× sucrose buffer (0.75 M sucrose, 10 mM NaCl, 2.5 mM $MgCl_2$, 10 mM Tris-Cl pH=7.4) was spiked to the homogenate and centrifuged at 800×*g* for 15 min to precipitate the cell nucleus. The supernatant was centrifuged at 10,000×*g* for 20 min to isolate the mitochondria. The pellet was washed twice with 1× sucrose buffer (0.25 M sucrose, 10 mM NaCl, 2.5 mM $MgCl_2$, 10 mM Tris-Cl pH=7.4) to reduce contamination from the abundant cytoplasmic proteins.

### Co-immunoprecipitation

The purified mitochondria from about $10^8$ cells were lysed with Triton X-100 lysis buffer (40 mM Tris, 120 mM NaCl, 1 % Triton X-100, 1 mM NaF, 1 mM $Na_3VO_4$) supplemented with protease inhibitor cocktail. The total protein

concentrations of the mitochondria lysates were measured with BCA assay. Rabbit anti-C1QBP polyclonal antibody was incubated with protein A beads at 4 °C for 1 h and conjugated to the beads with 450 μM DSS solution following the manufacturer's protocol. Next, C1QBP and its interacting proteins were purified with the antibody conjugated beads, followed by mass spectrometric analysis or Western blotting.

### SDS-PAGE, Western blotting, and in-gel digestion

Proteins were eluted from the beads by incubation with the SDS-PAGE loading buffer in boiling water bath for 10 min. For Western blotting, proteins separated by SDS-PAGE were transferred onto polyvinylidene fluoride membranes using a wet electro-blotter. The membranes were incubated with primary antibodies at 4 °C overnight and followed by incubation with secondary antibodies at room temperature for 1 h. Bound antibodies were detected by the ECL immunoblotting detection reagent. For in-gel digestion, the gels were first visualized using a silver staining kit following the manufacturer's protocol (Thermo Fisher Scientific, Waltham, MA). Each gel lane was divided into eight fractions and digested with trypsin before mass spectrometric analysis as described previously [17]. The normal IgG control samples were analyzed in parallel to distinguish the non-specific binding proteins.

### LC-MS/MS and data analysis

The tryptic peptides were analyzed using a nanoUPLC-ESI-LTQ Orbitrap mass spectrometer as described previously [17]. A nanoUPLC system (Waters, Milford, MA) was used to separate the tryptic peptides. Samples were loaded on a trap column and flushed with mobile phase A (0.1 % formic acid in $H_2O$) at 5 μL/min for 3 min before being delivered onto a nanoUPLC column (C18, 150×0.075 mm, 1.7 μm). The peptides were eluted using a 7–45 % B gradient (0.1 % formic acid in acetonitrile) over 90 min into a nano-electrospray ionization (nESI) LTQ Orbitrap mass spectrometer (Thermo Fisher Scientific, Waltham, MA). The mass spectrometer was operated in data-dependent mode in which an initial FT scan recorded the mass range of $m/z$ 350–2000, and the eight most abundant ions were automatically selected for collisional activated dissociation (CAD). The spray voltage was set as 2.0 kV. The normalized collision energy was set at 35 % for MS/MS. Raw data were searched against the Uniprot human protein database containing 98,778 sequence entries using the SEQUEST algorithm embedded in the Protein Discoverer 1.3 Software (Thermo Fisher Scientific, Waltham, MA). The following parameters were applied during the database search: 10 ppm precursor mass error tolerance, 1 Da fragment mass error tolerance, static modifications of carbamidomethylation for all cysteine residues, flexible modification of oxidation modifications for methionine residues, and one missed cleavage site of trypsin was allowed. FDR <0.01 was used as filtering criteria for all identified peptides. Only proteins identified with two or more unique peptides were considered, and proteins identified with the same set of peptides were grouped.

### Quantitative real-time polymerase chain reaction (qRT-PCR)

Total RNA was extracted from cells using the Trizol reagent (Invitrogen, Carlsbad, CA). Then, 1 μg total mRNA of each sample was used for reverse transcription with the Omniscript RT kit (Qiagen, Hilden, Germany). qRT-PCR was performed with a Roche FastStart Universal SYBR Green Master kit (Roche, Switzerland) according to the manufacturer's instructions. The primer sequences for C1QBP were 5′-AGTGCGGAAAGT-TGCCGGGGA-3′ (forward) and 5′-GAGCTCCACCAG- CTCATCTGC-3′ (reverse). GAPDH was used as the internal control and its primers were as follows: 5′-ACCACAGTC-CATGCCATCAC-3′ (forward) and 5′-TCCACCACCCTG-TTGCTGTA-3′ (reverse). Relative expression of C1QBP was normalized, and the data were analyzed using the $2^{-\Delta\Delta Ct}$ method.

### Immunofluorescence and confocal microscopy

Cells were plated in 12-well plates containing sterile glass coverslips, allowed to grow for 24 h. Cells were fixed with 4 % paraformaldehyde in PBS (pH 7.4) for 10 min at room temperature, permeabilized in 0.2 % Triton/PBS for 10 min and blocked in 3 % BSA in PBS for 1 h at room temperature. The cells were incubated with primary antibodies at 4 °C overnight, followed by staining with Alexa Fluor 488 and 546-conjugated secondary antibodies for 1 h at room temperature. MitoTracker (100 nM) was used for mitochondria staining. Coverslips were counter-stained with DAPI (1 ng/mL), mounted with ProLong® Gold antifade reagents and visualized with confocal laser scanning microscopy (Leica, Buffalo Grove, IL).

### Pyruvate dehydrogenase (PDH) enzyme activity assay

The PDH enzyme activities in the C1QBP overexpression and knockdown cells were measured using a dipstick assay kit purchased from Abcam (Cambridge, MA) following the manufacturer's protocol. Briefly, the cellular proteins were extracted using the sample buffer supplemented with detergent. Then 50 μL supernatant containing 160 μg cellular proteins was added to the activated dipstick and incubated for 60 min. The developed dipstick was washed, dried, and scanned using a photo scanner. All data were analyzed using the Image J software (http://rsb.info.nih.gov/ij/).

## Results and discussion

To investigate the mitochondrial interacting proteins of C1QBP, a subcellular fractionation coupled with CoIP-MS strategy was established. As shown in Fig. 1, cells were first homogenized to release the cellular organelles. Mitochondria were enriched by centrifugation and washed with the sucrose buffer to remove the contamination from abundant cytoplasmic proteins. Mitochondrial proteins were extracted using lysis buffer compatible for the downstream CoIP experiment. The anti-C1QBP antibody was conjugated to the surface of magnetic beads using DSS. Then the beads were incubated with mitochondrial extract to isolate C1QBP and its interacting proteins. IgG was used as negative control in this case and processed in parallel. The obtained immunoprecipitates were separated using SDS-PAGE, and each gel lane was divided into eight bands and digested with trypsin for LC-MS/MS analyses.

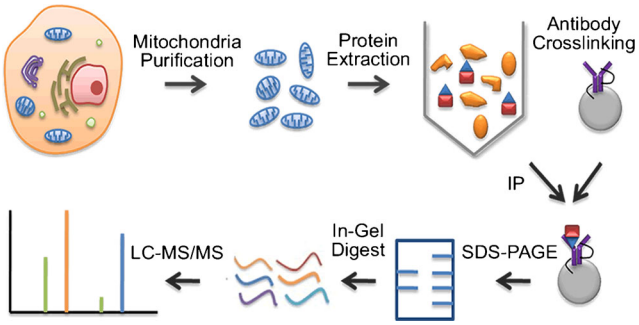


**Fig. 1** Overview of the experimental workflow. Cells were disrupted to release the cellular organelles. Mitochondria were enriched by centrifugation and washed with sucrose buffer. Mitochondrial proteins were extracted using lysis buffer containing 1 % Triton X-100. The anti-C1QBP antibody was conjugated to the surface of magnetic beads using DSS. The beads were incubated with mitochondrial extract to isolate C1QBP and its interacting proteins. The immunoprecipitates were separated using SDS-PAGE, and each gel lane was divided into eight bands and digested with trypsin for LC-MS/MS analyses

### Mitochondria purification

Mitochondrion is an important subcellular organelle for energy production through respiration. The number and size of mitochondria can vary greatly between different types of tissues and cells. Therefore, it is crucial to optimize the mitochondria isolation method to obtain high isolation efficiency and high purity for the specimen under investigation. Sucrose centrifugation is one of the most widely used methods for mitochondria purification. Here, we developed a modified mitochondria isolation method based on the protocol reported by Dimauro et al. [16]. HEK293T cells were first incubated with hypotonic buffer and disrupted to release the mitochondria. Three different methods were compared for cell homogenization, including sonication (Sonics, Newtown, CT), a 2-mL glass tissue homogenizer, and a syringe. For the HEK293 cells, the syringe was more effective for mitochondria isolation compared to the other two methods. The energy and duration of sonication had to be carefully optimized. The nucleus membrane was relatively fragile compared to other subcellular organelles, and nucleus protein contamination was observed in the cytoplasmic fraction. When the sonication energy was set too high, it would also destroy the mitochondria and cause mitochondrial protein loss (see Electronic Supplementary Material (ESM) Fig. S1). At the same time, incomplete cell disruption was commonly seen when using a tissue homogenizer. When using a homogenizer for subcellular fractionation, we recommend to centrifuge the cellular homogenate using a low centrifugation speed (~800 rpm) to remove the undisrupted cells before moving on to the mitochondria isolation in order to increase the purity of the obtained subcellular fractions. However, this step may cause low yield for mitochondria purification. It should be noted that this study mainly used HEK293T cells, and these three methods may perform differently when working on other types of cells.

Western blotting analysis was performed to evaluate the purity of the mitochondrial extract. As shown in Fig. 2a, the mitochondrial protein marker COX IV was only detected in the obtained mitochondrial fraction, while the cytosolic protein marker β-actin was only observed in the cytoplasmic fraction. BCA assay was used to analyze the protein amount in the mitochondrial protein extract. As shown in Fig. 2b, based on five independent experiments, the relative amount

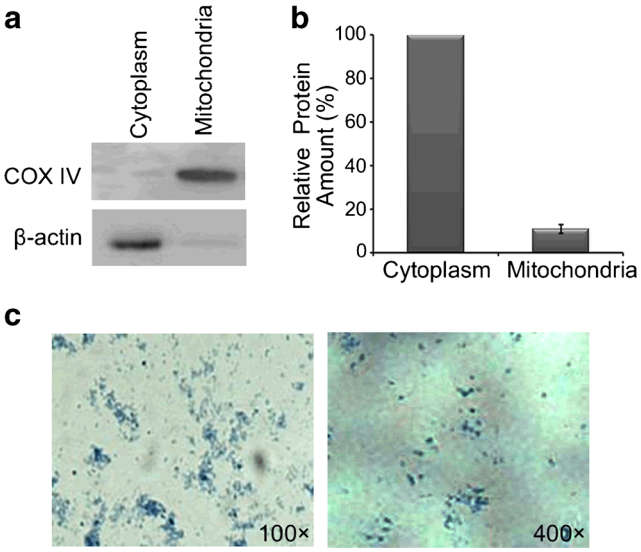


**Fig. 2** Evaluation of the mitochondria purification. **a** Western blot of the mitochondrial and cytoplasmic fractions. COX IV and β-actin were used as specific protein markers for mitochondria and cytoplasm, respectively. **b** BCA analysis of the relative protein amount in the mitochondrial extracts as compared with the cytoplasmic fractions. The value was expressed as mean±SD of five independent experiments. **c** Bright-field microscopy images of the purified mitochondria. Mitochondria were stained using Janus Green B

of proteins in the purified mitochondria was measured to be around 12 % as compared to the cytoplasmic fractions. The purity of the isolated mitochondria was further examined under the microscope using Janus Green B staining, and individual oval-shaped particles stained with blue color were observed (Fig. 2c).

### Isolation of the C1QBP interacting proteins from the mitochondria extract

Isolation of the C1QBP interacting proteins from the mitochondria was technically challenging. At first, no protein of interest was detected using a conventional co-immunoprecipitation protocol, where anti-C1QBP antibody was incubated with the mitochondrial extract and then purified by protein A agarose beads. Broad bands of IgG light chain and heavy chain were observed, interfering with the analysis of the potential interacting proteins (Fig. 3a). To reduce the interference from the antibody, crosslinker DSS was used to conjugate the antibody to the protein A beads. As shown in Fig. 3b, conjugating IgG to the protein A beads using DSS greatly reduced the co-elution of IgG and the overall sample background. The use of agarose beads and magnetic beads was also compared. The sample background of agarose beads and magnetic beads were compared in three conditions: without normal IgG, with normal IgG, and with normal IgG crosslinked to the beads. As shown in Fig. 3b, slightly darker background was observed for agarose beads when incubated with the cell lysates without IgG as compared to the magnetic beads, indicating that more cellular proteins bind non-specifically with the agarose beads. Loading IgG to the beads further increased the sample background. Some of these proteins may originate from the IgG sample, and it was also possible that some cellular proteins could non-specifically bind with IgG. Although the same amount of IgG was used, more IgG was loaded onto the magnetic beads, probably because of their larger surface to volume ratio, resulting in higher capacity for antibody uptake. Collectively, using magnetic beads and DSS crosslinking provided relatively higher antibody loading capacity and lower sample background compared to the agarose beads.

### DLAT was identified as a novel mitochondrial C1QBP interacting protein

By optimizing the CoIP condition, the purity of the C1QBP mitochondrial immunoprecipitates was improved. As shown in Fig. 3a, the IgG interference was reduced and a clear band around 70 kDa was observed from the C1QBP immunoprecipitates. The whole gel lane was divided into eight fractions and in-gel digested for LC-MS/MS analysis. Control IgG samples were also analyzed in parallel to distinguish the background proteins. Only 80 proteins were observed in the IgG control (see ESM Table S1), and most of them were keratin contaminates induced during the in-gel digestion. The most abundant non-specific binding protein from the mitochondria is the stress-70 protein, mitochondrial (HSPA9). After excluding all the background interfering proteins, only one protein, DLAT, was identified as a potential C1QBP interacting protein. DLAT was identified from the mitochondrial C1QBP immunoprecipitates with three unique peptides, and two representative MS/MS spectra are shown in Fig. 4. Compared to the previous study of C1QBP interacting proteins [14], much fewer proteins were detected in the C1QBP mitochondrial immunoprecipitates suggesting that C1QBP may present in the mitochondria as a matrix molecule and only bind with other proteins at low level or transiently. When using whole cell lysate for co-immunoprecipitation, the abundant interacting proteins from the cytoplasm suppressed the detection of mitochondrial proteins with low abundance. The results indicate that the detection sensitivity of mitochondrial C1QBP interacting proteins is increased by isolating the mitochondria before LC-MS/MS analyses.

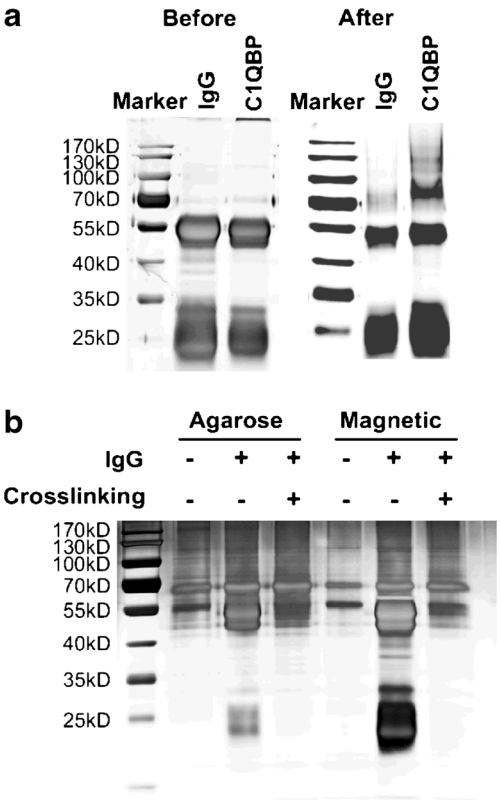


**Fig. 3** Purification of C1QBP interacting proteins using co-immunoprecipitation. **a** Optimization of the co-immunoprecipitation procedure. SDS-PAGE separation of the C1QBP immunoprecipitates obtained from the mitochondria before (*left*) and after (*right*) method optimization. The gel was visualized using silver staining. **b** Protein A agarose beads and magnetic beads were compared. Anti-C1QBP antibody was crosslinked with the beads using 450 μM DSS in PBS

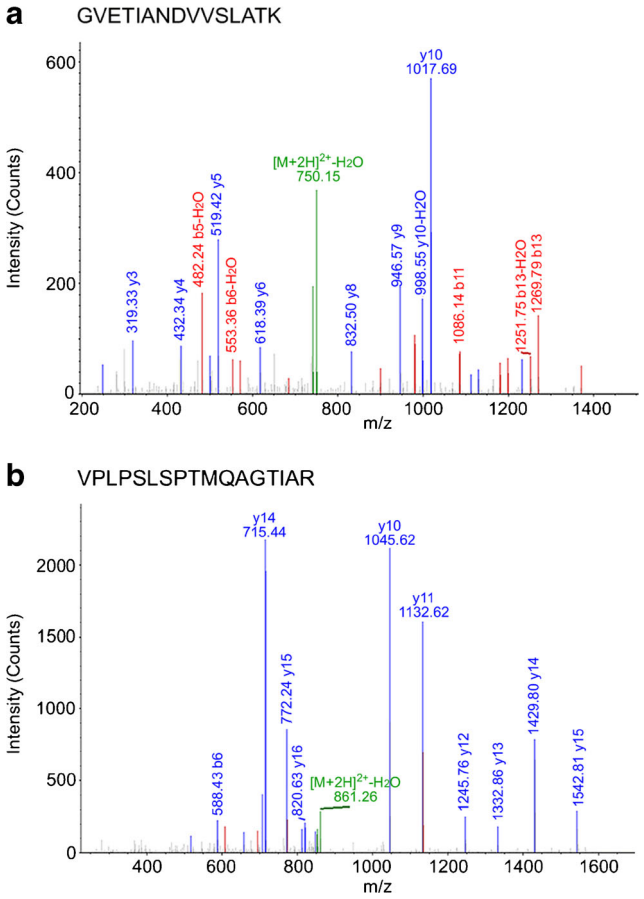


**Fig. 4** Identification of the mitochondrial C1QBP interacting protein DLAT. Representative MS/MS spectra of the tryptic peptides from DLAT: **a** GVETIANDVVSLATK and **b** VPLPSLSPTMQAGTIAR. The b and y ions were indicated with *red* and *blue colors*, respectively

## C1QBP interacts with DLAT and regulates the enzyme activity of pyruvate dehydrogenase

Western blotting and confocal microscopy analyses were used to further verify the interactions between C1QBP and DLAT. As shown in Fig. 5a, reciprocal interaction between DLAT and C1QBP was observed using co-immunoprecipitation and Western blotting analysis. Confocal immunofluorescence analysis suggested that C1QBP located in the mitochondria as indicated with MitoTracker (Fig. 5b), and DLAT colocalized with C1QBP in the mitochondria.

DLAT is the core component of the pyruvate dehydrogenase (PDH) complex, a pivotal enzyme catalyzing the conversion of pyruvate to acetyl-CoA. The synthesized acetyl-CoA is used in the tricarboxylic acid (TCA) cycle to generate energy [18]. To investigate the biological implication of the interaction between C1QBP and DLAT, the PDH enzyme activity was measured in cells with different expression levels of C1QBP. Two different types of renal cancer cell lines were examined, including 786-O and ACHN. As shown in Fig. 6, the PDH enzyme activity in the 786-O-C1QBP cells was increased by about 30 % compared to the vector control, and the depletion of C1QBP reduced the PHD enzyme activity by about 45 %. Similar results were also observed in the ACHN cells. These results show that C1QBP can positively regulate the enzyme activity of PDH in renal cancer cells.

One of the most well-recognized functions of C1QBP in the mitochondria is to regulate oxidative phosphorylation (OXPHOS). Fogal et al. have reported that knocking down the expression of C1QBP in breast cancer cells could shift the metabolism from OXPHOS to glycolysis [19]. Most cancer cells are believed to rely more on glycolysis for energy production even when oxygen is adequate for mitochondrial respiration [20]. Such metabolism shift is important for the cancer cells to maintain the increased anabolic requirements for cell proliferation [21, 22]. Although mitochondrial respiration is believed to be reduced in cancer cells, the continued mitochondrial function is still required for cancer cell survival. The balance between OXPHOS and glycolysis is essential for the development, progression, and metastasis of tumor cells [9]. It

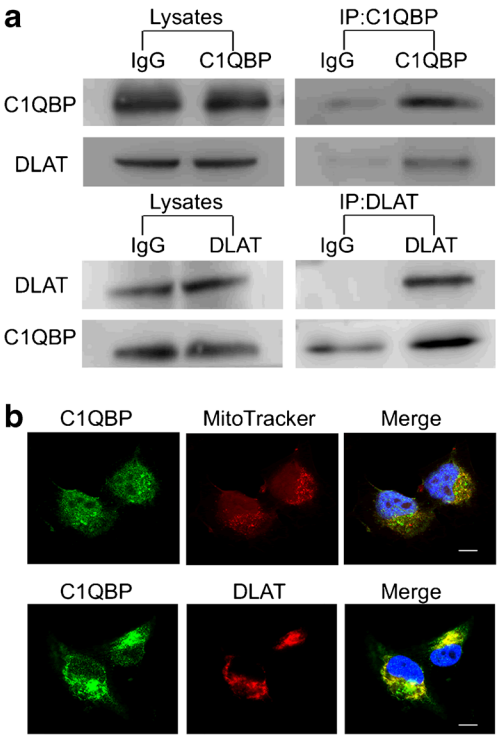


**Fig. 5** Validation of the newly discovered mitochondrial C1QBP interacting protein. **a** The mitochondrial immunoprecipitates of C1QBP were purified using rabbit anti-C1QBP polyclonal antibody conjugated Protein A magnetic beads and separated with SDS-PAGE. The presence of DLAT was analyzed by Western blotting. Normal rabbit IgG was used as the negative control. The mitochondrial immunoprecipitates of DLAT were purified using anti-DLAT mouse monoclonal antibody conjugated Protein G magnetic beads and separated with SDS-PAGE. The presence of DLAT and C1QBP was analyzed by Western blotting. Normal rabbit or mouse IgG was used as the negative control. **b** Confocal microscopy analysis showed that endogenous C1QBP colocalized with DLAT in the mitochondria of HEK293T cells. The cell nucleus was stained with DAPI and the mitochondria were visualized using MitoTracker. The *scale bars* were 10 μm

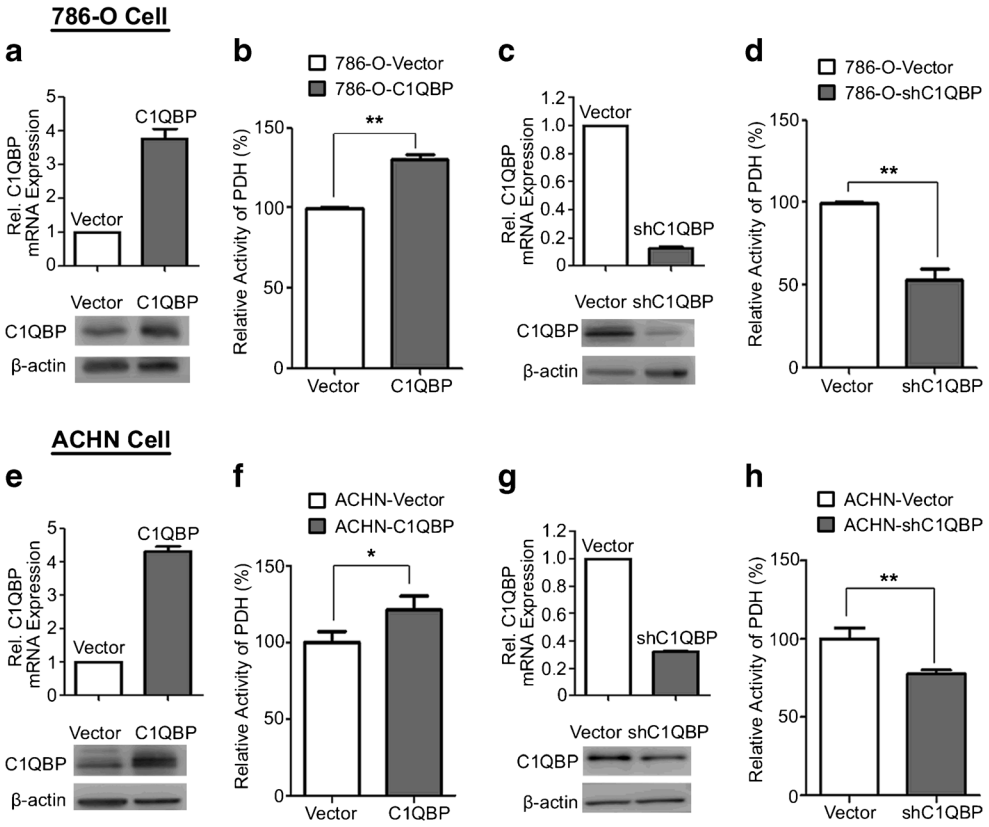


**Fig. 6** C1QBP regulates PDH enzyme activity in renal cancer cells. C1QBP was overexpressed in the 786-O cells (**a**) and ACHN cells (**e**) by infection with C1QBP lentivirus plasmid, and the expression level of C1QBP was examined using real-time PCR (*upper panel*) and Western blotting (*lower panel*). The PDH enzyme activities in the 786-O-C1QBP cells (**b**) and ACHN-C1QBP cells (**f**) were measured using the dipstick assay and compared with the vector control. C1QBP was depleted from the 786-O cells (**c**) and ACHN cells (**g**), and the knockdown of C1QBP was validated using real-time PCR (*upper panel*) and Western blotting (*lower panel*). The PDH enzyme activities in the 786-O-shC1QBP cells (**d**) and ACHN-shC1QBP cells (**h**) were measured using the dipstick assay and compared with the vector control. The quantitative data were expressed as means±SD of three independent experiments. Statistical analysis was performed via one-way analysis of variance (*$p \leq 0.05$, **$p \leq 0.01$)

has been suggested that C1QBP could regulate OXPHOS through regulating the expression of multiple mitochondrial-DNA-encoded OXPHOS enzymes [19]. However, it was not clear whether C1QBP could also directly regulate their functions through protein-protein interactions. Our findings suggest that C1QBP might regulate OXPHOS through binding to DLAT, providing a novel molecular mechanism to explain the role of C1QBP in the regulation of cellular respiration. Further studies will be conducted to confirm such conjecture and to understand the roles of C1QBP in the balance of tumor metabolism.

## Conclusion

In this study, subcellular fractionation was combined with CoIP-MS to characterize protein-protein interactions in the mitochondria. Using this method, DLAT was characterized as a novel mitochondrial C1QBP binding protein, unveiling a potential new role of C1QBP in the mitochondria. This study demonstrates that the subcellular fractionation coupled with CoIP-MS is effective to study the protein-protein interactions in the mitochondria. Such a strategy could be easily adapted to analyze subcellular protein-protein interactions for other proteins of interest. Furthermore, unlike the traditional CoIP-MS, this method retains the protein localization information, providing more insights regarding the biological implications of the detected protein-protein interactions.

**Acknowledgments** This work was supported by grants from National Natural Science Foundation of China (21575103, 21205088, 81472683 and 81201871), National High Technology Research and Development Program 863 (2015AA020403), Tianjin Innovation Team Program (TD12-5025), National Science Fund for Distinguished Young Scholars (81125019), Doctoral Research Fund from the Ministry of Education of China (20121202120001).

**Compliance with ethical standards**

**Conflict of interest** The authors declare that they have no competing interests.

## References


1. Miteva YV, Budayeva HG, Cristea IM (2013) Proteomics-based methods for discovery, quantification, and validation of protein-protein interactions. Anal Chem 85(2):749–68
2. Ngounou WA, Sokolowska I, Woods AG, Roy U, Deinhardt K, Darie CC (2014) Protein-protein interactions: switch from classical methods to proteomics and bioinformatics-based approaches. Cell Mol Life Sci 71(2):205–28
3. Blagoev B, Kratchmarova I, Ong SE, Nielsen M, Foster LJ, Mann M (2003) A proteomics strategy to elucidate functional protein-protein interactions applied to EGF signaling. Nat Biotechnol 21(3):315–8
4. Guerrero C, Milenkovic T, Przulj N, Kaiser P, Huang L (2008) Characterization of the proteasome interaction network using a QTAX-based tag-team strategy and protein interaction network analysis. Proc Natl Acad Sci U S A 105(36):13333–8
5. Krainer AR, Mayeda A, Kozak D, Binns G (1991) Functional expression of cloned human splicing factor SF2: homology to RNA-binding proteins, U1 70K, and Drosophila splicing regulators. Cell 66(2):383–94
6. Gupta S, Batchu RB, Datta K (1991) Purification, partial characterization of rat kidney hyaluronic acid binding protein and its localization on the cell surface. Eur J Cell Biol 56(1):58–67
7. Ghebrehiwet B, Lim BL, Peerschke EI, Willis AC, Reid KB (1994) Isolation, cDNA cloning, and overexpression of a 33-kD cell surface glycoprotein that binds to the globular "heads" of C1q. J Exp Med 179(6):1809–21
8. Peerschke EI, Ghebrehiwet B (2007) The contribution of gC1qR/p33 in infection and inflammation. Immunobiology 212(4–5):333–42
9. Dang CV (2010) p32 (C1QBP) and cancer cell metabolism: is the Warburg effect a lot of hot air? Mol Cell Biol 30(6):1300–2
10. Majumdar M, Meenakshi J, Goswami SK, Datta K (2002) Hyaluronan binding protein 1 (HABP1)/C1QBP/p32 is an endogenous substrate for MAP kinase and is translocated to the nucleus upon mitogenic stimulation. Biochem Biophys Res Commun 291(4):829–37
11. Chen YB, Jiang CT, Zhang GQ, Wang JS, Pang D (2009) Increased expression of hyaluronic acid binding protein 1 is correlated with poor prognosis in patients with breast cancer. J Surg Oncol 100(5): 382–6
12. Chen R, Wang Y, Liu Y, Zhang Q, Zhang X, Zhang F et al (2013) Quantitative study of the interactome of PKCzeta involved in the EGF-induced tumor cell chemotaxis. J Proteome Res 12(3):1478–86
13. Kim KB, Yi JS, Nguyen N, Lee JH, Kwon YC, Ahn BY et al (2011) Cell-surface receptor for complement component C1q (gC1qR) is a key regulator for lamellipodia formation and cancer metastasis. J Biol Chem 286(26):23093–101
14. Zhang X, Zhang F, Guo L, Wang Y, Zhang P, Wang R et al (2013) Interactome analysis reveals that C1QBP (complement component 1, q subcomponent binding protein) is associated with cancer cell chemotaxis and metastasis. Mol Cell Proteomics 12(11):3199–209
15. Soltys BJ, Kang D, Gupta RS (2000) Localization of P32 protein (gC1q-R) in mitochondria and at specific extramitochondrial locations in normal tissues. Histochem Cell Biol 114(3):245–55
16. Dimauro I, Pearson T, Caporossi D, Jackson MJ (2012) A simple protocol for the subcellular fractionation of skeletal muscle cells and tissue. BMC Res Notes 5:513–7
17. Wang Y, Yue D, Xiao M, Qi C, Chen Y, Sun D et al (2015) C1QBP negatively regulates the activation of oncoprotein YBX1 in the renal cell carcinoma as revealed by interactomics analysis. J Proteome Res 14(2):804–13
18. Patel MS, Nemeria NS, Furey W, Jordan F (2014) The pyruvate dehydrogenase complexes: structure-based function and regulation. J Biol Chem 289(24):16615–23
19. Fogal V, Richardson AD, Karmali PP, Scheffler IE, Smith JW, Ruoslahti E (2010) Mitochondrial p32 protein is a critical regulator of tumor metabolism via maintenance of oxidative phosphorylation. Mol Cell Biol 30(6):1303–18
20. Koppenol WH, Bounds PL, Dang CV (2011) Otto Warburg's contributions to current concepts of cancer metabolism. Nat Rev Cancer 11(5):325–37
21. Vander Heiden MG, Cantley LC, Thompson CB (2009) Understanding the Warburg effect: the metabolic requirements of cell proliferation. Science 324(5930):1029–33
22. Hitosugi T, Chen J (2014) Post-translational modifications and the Warburg effect. Oncogene 33(34):4279–85
23. Vizcaíno JA, Deutsch EW, Wang R, Csordas A, Reisinger F, Ríos D et al (2014) ProteomeXchange provides globally co-ordinated proteomics data submission and dissemination. Nat Biotechnol 30(3): 223–6